Divergent Pathogenesis and Transmission of Highly Pathogenic Avian Influenza A(H5N1) in Swine

Bailey Arruda, Amy L. Vincent Baker, Alexandra Buckley, Tavis K. Anderson, Mia Torchetti, Nichole Hines Bergeson, Mary Lea Killian, Kristina Lantz

Highly pathogenic avian influenza (HPAI) viruses have potential to cross species barriers and cause pandemics. Since 2022, HPAI A(H5N1) belonging to the goose/Guangdong 2.3.4.4b hemagglutinin phylogenetic clade have infected poultry, wild birds, and mammals across North America. Continued circulation in birds and infection of multiple mammalian species with strains possessing adaptation mutations increase the risk for infection and subsequent reassortment with influenza A viruses endemic in swine. We assessed the susceptibility of swine to avian and mammalian HPAI H5N1 clade 2.3.4.4b strains using a pathogenesis and transmission model. All strains replicated in the lung of pigs and caused lesions consistent with influenza A infection. However, viral replication in the nasal cavity and transmission was only observed with mammalian isolates. Mammalian adaptation and reassortment may increase the risk for incursion and transmission of HPAI viruses in feral, backyard, or commercial swine.

Influenza A viruses (IAV) of avian and swine origin have caused 5 pandemics in the previous 2 centuries (*1*). Aquatic avian populations, the primary reservoir for IAV, harbor numerous virus subtypes (H1–16), to which mammals have minimal preexisting immunity (*2*). Among those subtypes, H5 avian influenza virus infections have been documented in domestic poultry, humans, marine mammals, and swine, among others (*3*–*6*).

Over the past decade, H5NX highly pathogenic avian influenza (HPAI) viruses belonging to the goose/Guangdong (Gs/GD) 2.3.4.4 hemagglutinin (HA) phylogenetic clade have caused infections in wild birds and poultry, resulting in major mortality events and spread to >84 countries, and were recognized as a panzootic (*7*,*8*). In addition, evidence exists of enzootic HPAI virus maintenance in Europe, further signifying a paradigm shift in the biology of HPAI (*9*). Since February 2022, HPAI H5N1 clade 2.3.4.4b virus originating from a trans-Atlantic incursion has caused outbreaks across North America, resulting in >77 million poultry deaths, extensive deaths in wild bird species, and unprecedented disease in wild mammals (*4*–*6*,*10*)

The transcontinental circulation of clade 2.3.4.4b viruses within bird populations continues to enable reassortment with low pathogenicity avian influenza (LPAI) viruses and resulted in the emergence of numerous genotypes of potentially different phenotypes (*11*,*12*). Furthermore, interspecies transmission between avian species and peridomestic mammals has resulted in viruses with mammalian adaptation markers that pose a public health risk should they gain efficient transmission among mammals. A subset of HPAI H5NX clade 2.3.4.4 viruses bound both α2,6-linked (human) and α2,3-linked (avian) sialic acid receptors (*13*–*16*). Furthermore, nearly half of mammal isolates of HPAI H5N1 clade 2.3.4.4b acquired mammalian adaptation markers (E627K, D701N, or T271A substitutions) in the polymerase basic (PB) 2 protein (*1*,*17*). In addition, the HPAI H5N1 viruses collected during an outbreak in farmed mink contained mutations in the neuraminidase protein that caused disruption of the second sialic acid binding site, a feature typical of human-adapted IAV (*17*). During January 2022–April 17, 2023, a total of 8 reported human cases of H5N1 influenza from clade 2.3.4.4b occurred, many severe or fatal (*4*,*18*). Those characteristics of the current clade 2.3.4.4b H5 HPAI elevate the potential for human infection and adaptation.

Author affiliations: Agriculture Research Service, Ames, Iowa, USA (B. Arruda, A.L. Vincent Baker, A. Buckley, T.K. Andersen); Animal and Plant Health Inspection Service, Ames (M. Torchetti, N. Hines Bergeson, M.L. Killian, K. Lantz)

DOI: https://doi.org/10.3201/eid3004.231141

Table 1. Virus strain accession number, genotype, constellation, and reassorted genes in study of divergent pathogenesis and transmission of highly pathogenic avian influenza A(H5N1) in swine*

Strain	GISAID accession no.†	Genotype	Constellation (PB2|PB1|PA|HA|NP|NA|M|NS)	Reassorted genes
A/turkey/Minnesota/22-010654-001/2022	16555202	B2.1	am1.2|ea1|ea1|ea1|am1.1|ea1|ea1|ea1	PB2, NP
A/bald eagle/Florida/W22-134-OP/2022	15063846	B1.1	am1.1|am1.1|ea1|ea1|am1.2|ea1|ea1|ea1	PB2, PB1, NP
A/raccoon/Washington/22-018406-002/2022	15078252	B2.1	am1.2|ea1|ea1|ea1|am1.1|ea1|ea1|ea1	PB2, NP
A/red fox/Michigan/22-018712-001/2022	15078253	B3.2	am2.1|am1.2|ea1|ea1|am1.4.1|ea1|ea1|am1.1	PB2, PB1, NP, NS

*am, American; ea, Eurasian; PB2, polymerase basic 2; PB1, polymerase basic 1; PA, polymerase acidic; HA, hemagglutinin; NP, nucleoprotein; NA, neuraminidase; M, matrix protein 1; NS, non-structural protein 1.
†GISAID, https://www.gisaid.org.

A longstanding dogma of IAV biology identified swine as a mixing vessel and vital to the emergence of human pandemic IAV by supporting reassortment that could lead to antigenic shift (*1*). However, at a receptor level, swine might be no more susceptible to infection by avian IAVs than humans (*1*). Mammalian adaption of HPAI is a multigenic trait, and the genetic changes necessary for H5N1 strains to adapt to swine and acquire efficient and sustained transmissibility are poorly understood. However, swine-adapted IAV have a propensity for evolution through polymerase errors and reassortment, followed by spread of mutated or reassorted strains through contact among densely housed commercial pigs and pig transport. If an avian IAV strain, such as H5Nx 2.3.4.4b, successfully infected domestic swine, pig-to-pig transmission, reassortment with endemic swine IAV, or acquisition of adaptive mutations that might enable an avian-to-mammalian switch could potentially occur (*1*). Continued circulation in the wild bird population

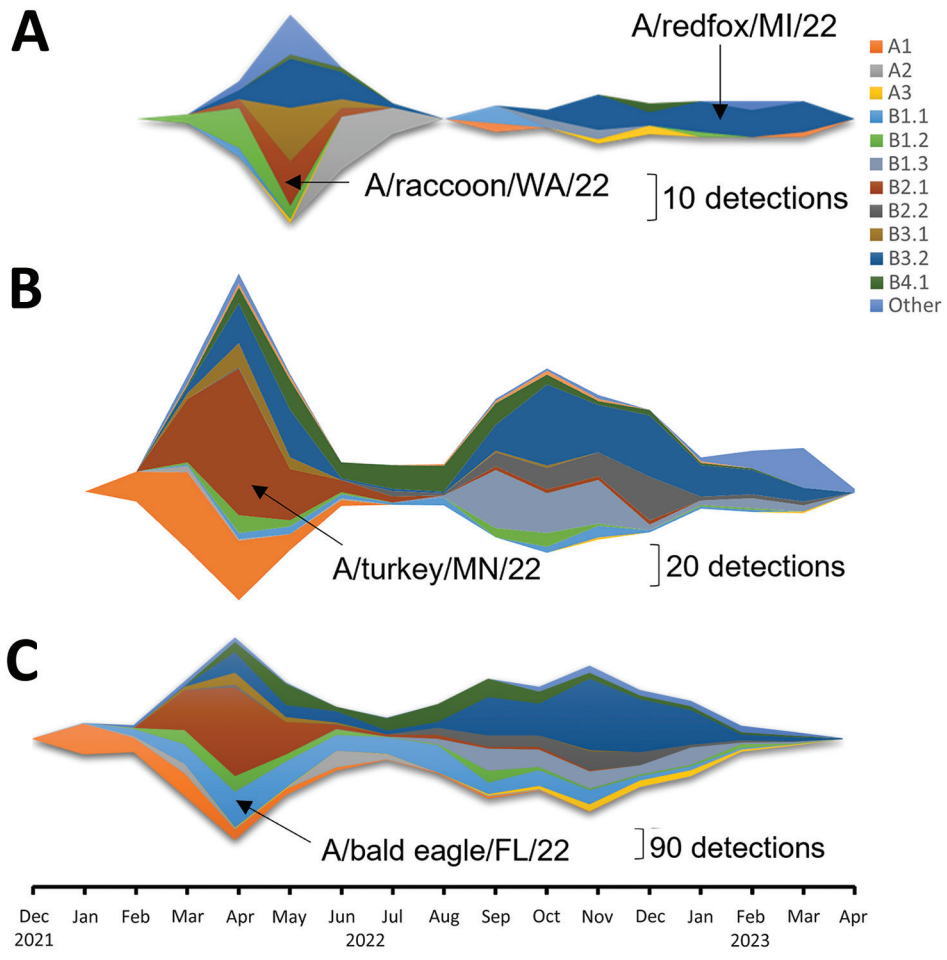

Figure 1. Detection of Eurasian lineage goose/Guangdong H5 clade 2.3.4.4b virus and identification of virus isolates used in study of divergent pathogenesis and transmission of highly pathogenic avian influenza A(H5N1) in swine, by genotype. A) Wild mammal; B) poultry; C) wild birds.

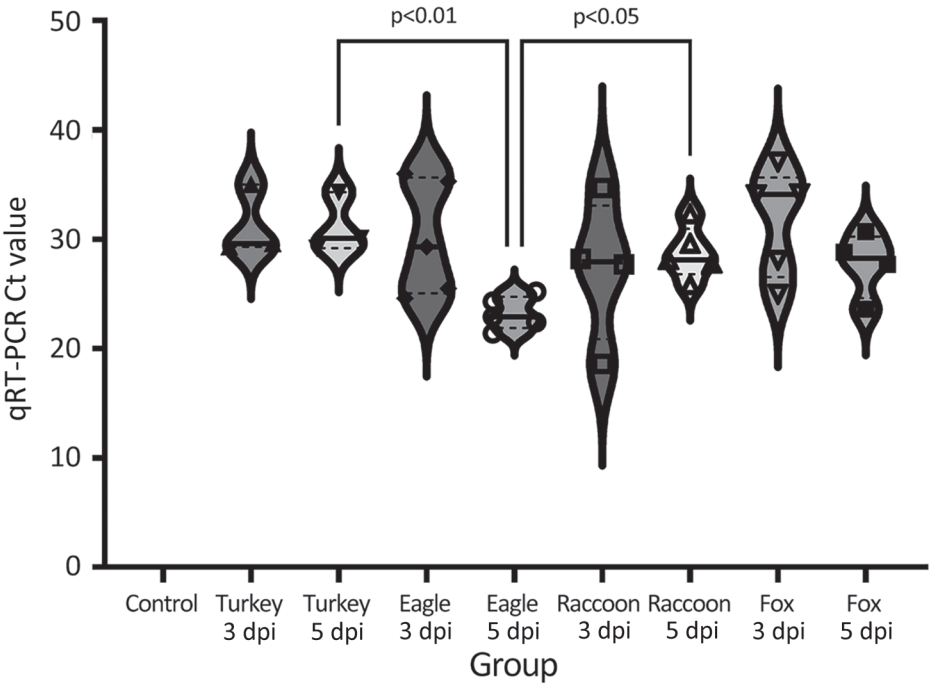

Figure 2. Violin plots showing Ct values for bronchoalveolar lavage fluid from pigs, by virus strain and dpi, in study of divergent pathogenesis and transmission of highly pathogenic avian influenza A(H5N1) in swine. Values were determined by quantitative reverse transcription PCR (ThermoFisher Scientific, https://www.thermofisher.com). All strains replicated in the lung of pigs. No statistical difference was detected between strains by dpi. Solid lines within plots indicate medians, dashed lines indicate quartiles, and symbols indicate individual pig values. dpi, days postinoculation; Eagle 3 dpi, A/bald eagle/FL/22 necropsied on 3 dpi; Eagle 5 dpi, A/bald eagle/FL/22 necropsied at 5 dpi; Fox 3 dpi, A/redfox/MI/22 necropsied at 3 dpi; Fox 5 dpi, A/redfox/MI/22 necropsied at 5 dpi; Raccoon 3 dpi, A/raccoon/WA/22 necropsied at 3 dpi; Racoon 5 dpi, A/raccoon/WA/22 necropsied at 5 dpi; Turkey 3 dpi, A/turkey/MN/22 necropsied at 3 dpi; Turkey 5 dpi, A/turkey/MN/22 necropsied at 5 dpi.

and peridomestic wild mammal infections elevate the risk for exposure of swine because of the current outbreak's wide distribution in states with large pig populations. To address concerns over susceptibility of swine to HPAI H5N1 clade 2.3.4.4b virus detected in the United States and to elucidate potential molecular mutations associated with H5N1 replication and transmission in swine, we conducted a study with 4 strains representing 3 different genotypes in a pig pathogenesis and transmission model. This information is key to building awareness and detection capabilities in the swine sector, as well as to informing risk assessments and early warning systems to safeguard human health.

Materials and Methods

Viruses

We evaluated the pathogenicity and transmission in crossbred, 4-week-old pigs of 4 strains of the 2022 spring HPAI H5N1 clade 2.3.4.4b outbreak: A/turkey/Minnesota/22–010654-001/2022 (A/turkey/MN/22), A/bald eagle/Florida/W22-134-OP/2022 (A/bald eagle/FL/22), A/raccoon/Washington/22-018406-002/2022 H5N1 (A/raccoon/WA/22) and A/redfox/Michigan/22-018712-001/2022 (A/redfox/MI/22). Those 4 strains resulted from Eurasian avian HPAI H5N1 clade 2.3.4.4b reassortment with North American LPAI lineage internal genes and represented 3 different reassortment patterns frequently detected among H5N1 strains during 2022 (Table 1; Figure 1) (Appendix 1, https://wwwnc.cdc.gov/EID/article/30/4/23-1141-App1.pdf). Both the A/raccoon/WA/22 and the A/redfox/MI/22 strains contained the PB2 E627K mammalian adaptation mutation.

Virus Propagation and Titration

We conducted the study in compliance with the Animal Care and Use Committee of the US Department of Agriculture—Agricultural Research Service National Animal Disease Center under Biosafety Level 3 guidelines, including enhancements required by the Federal Select Agent Program. We passaged virus stocks in 10-day-old embryonating chicken eggs, harvested the allantoic fluid from infected eggs, divided it into aliquots, and stored it at –70°C until use. We determined viral titers by using MDCK cells according to standard methods (*19*).

Swine Pathogenesis and Transmission Study

We blocked 88 pigs by litter and randomly allocated them into a negative control group or a group of 20 (1 group per virus strain). We inoculated 15 pigs per virus strain intranasally with 1 ml (0.5 ml per

nostril) of ≈10^5 50% tissue culture infective dose/mL using a Nasal Intranasal Mucosal Atomization Device (Teleflex, https://www.teleflex.com). We comingled 5 naive contact pigs with each of the virus-inoculated groups at 2 days postinoculation (dpi). We collected nasal swabs from inoculated pigs and contact pigs on 0, 1, 3, 5, and 7 dpi or days postcontact (dpc). We necropsied 5 inoculated pigs per group at 3, 5, and 14 or 17 dpi and the 5 contact pigs at 12 or 15 dpc. We collected bronchoalveolar lavage fluid (BALF) at necropsy on 3 and 5 dpi. We also obtained serum samples at necropsy (Appendix 1). We necropsied 8 negative control pigs from the same source herd as inoculated and contact pigs on ≈5 DPI to evaluate health status and background respiratory tract lesions.

Viral RNA Detection and Serology

We extracted viral RNA from nasal swab and BALF samples by using the MagMax Viral RNA isolation kit (ThermoFisher Scientific, https://www.thermofisher.com) and subjected it to real-time reverse transcription assays targeting multiple genes of IAV and a H5 2.3.4.4-specific HA gene (*20*). Cycle threshold (Ct) value for IAV quantitative reverse transcription PCR (qRT-PCR) interpretation was according to manufacturer's suggestion: Ct value of <38 indicated the sample was positive, Ct value of 38–40 indicated the sample was suspect; if undetected, the sample was negative. We determined seroconversion by using an IAV nucleoprotein (NP)–blocking ELISA (IDEXX, https://www.idexx.com).

Positive Sample Metagenomic Sequencing and Analyses

We amplified IAV RNA from samples as described (*10*). For each of the samples, we conducted variant calling by trimming raw FASTQ files using Trimmomatic (http://www.usadellab.org/cms/?page=trimmomatic) with a sliding window size of 5 bp and a minimum Q-score of 30, discarding reads that were trimmed to a length <100 bases. We aligned reads to reference sequences using bowtie2 version 2.3.2 (https://sourceforge.net/projects/bowtie-bio/files/bowtie2/2.3.2) and removed duplicate reads were removed using Picard (https://broadinstitute.github.io/picard). We converted the BAM files to mpileup using samtools (https://www.htslib.org) and identified within-host variants using VarScan (https://varscan.sourceforge.net). For a variant to

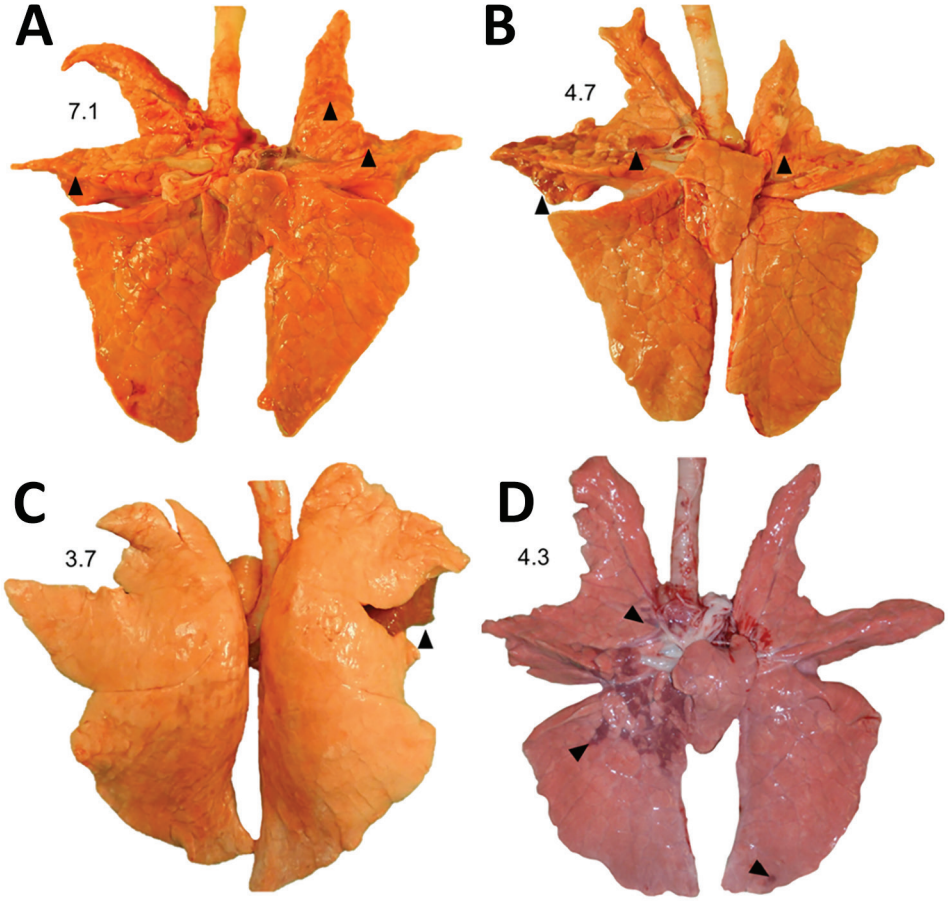

Figure 3. Macroscopic lung lesions and respective weighted macroscopic lung score of swine infected with highly pathogenic avian influenza A(H5N1) virus belonging to the goose/Guangdong 2.3.4.4b hemagglutinin phylogenetic clade. A) Multifocal pulmonary consolidation (arrowheads) in pig 777 infected with A/turkey/MN/22, necropsied at 3 days postinoculation (dpi). B) Multifocal pulmonary consolidation (arrowheads) in pig 796 infected with A/bald eagle/FL/22 necropsied on 5 dpi. C) Locally extensive pulmonary consolidation (arrowheads) in pig 58 infected with A/raccoon/WA/22 necropsied on 3 dpi. D) Multifocal pulmonary consolidation (arrowheads) of pig 78 infected with A/redfox/MI/22 necropsied on 3 dpi.

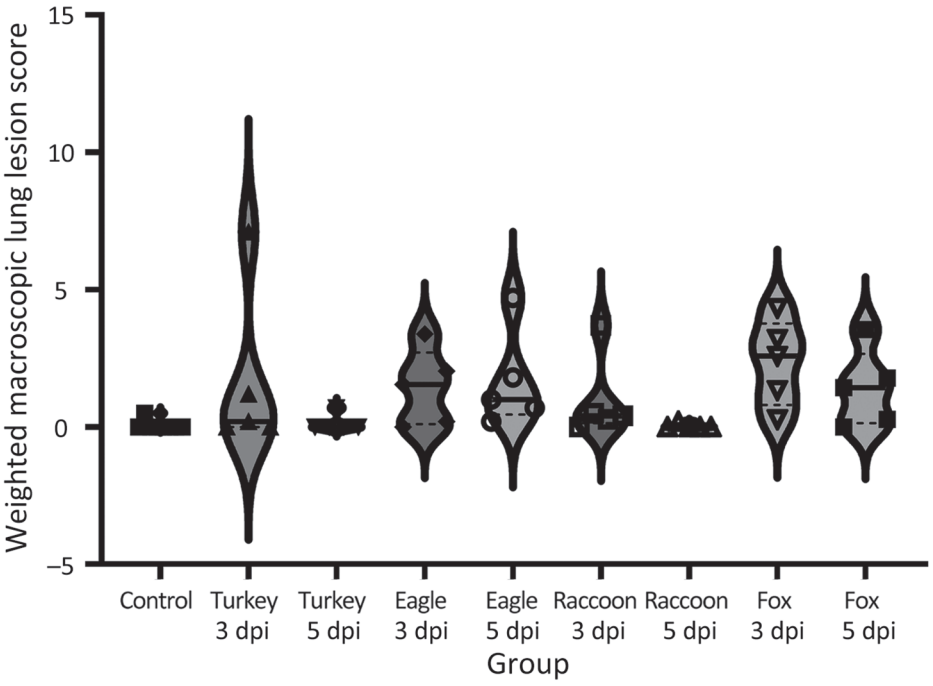

Figure 4. Violin plots of weighted macroscopic lung scores, by virus strain and dpi, of swine infected with highly pathogenic avian influenza A(H5N1) virus belonging to the goose/Guangdong 2.3.4.4b hemagglutinin phylogenetic clade. All strains caused macroscopic lesions consistent with influenza A virus infection in ≥1 pig. Solid lines within plots indicate medians, dashed lines indicate quartiles, and symbols indicate individual pig values. No statistically significant differences were detected between strains by dpiI. dpi, days postinoculation; eagle 3 dpi, A/bald eagle/FL/22 necropsied at 3 dpi; eagle 5 dpi, A/bald eagle/FL/22 necropsied at 5 dpi; fox 3 dpi, A/redfox/MI/22 necropsied at 3 dpi; fox 5 dpi, A/redfox/MI/22 necropsied at 5 dpi; raccoon 3 dpi, A/raccoon/WA/22 necropsied at 3 dpi; raccoon 5 dpi, A/raccoon/WA/22 necropsied at 5 dpi; turkey 3 dpi, A/turkey/MN/22 necropsied at 3 dpi; turkey 5 dpi, A/turkey/MN/22 necropsied at 5 dpi.

be reported, we required the sequencing depth to be 100×, PHRED quality scores to be 30, and detection frequency to be ≥1%. We compiled all reported variant calls and raw FASTQ files (https://github.com/flu-crew/datasets). We used the Sequence Feature Variant Types tool from the Influenza Research Database to download all currently available annotations for H5 HA, N1 neuraminidase, and the remaining internal genes (*21*). For each genome, we computed nucleotide diversity using the synonymous (π_S) and nonsynonymous (π_N) diversity calculations in SNPGenie (https://github.com/chasewnelson/SNPGenie) with a minimum allele frequency cutoff set to 1% (*22*) (Appendix 1).

Macroscopic and Microscopic Lesion Score

At necropsy, we recorded the percentage of affected surface area per lung lobe and used that to calculate a weighted macroscopic lung lesion score (*23*). We fixed tissue samples from the trachea and right middle or affected lung lobe in 10% buffered formalin for histologic examination and transferred to 70% ethanol after 48 hours. A veterinary pathologist blinded to treatment evaluated microscopic lesions of the lung and trachea (Appendix 1).

Immunohistochemistry

We conducted immunohistochemistry (IHC) staining manually on 5-µm–thick sections using a rabbit polyclonal anti-influenza A NP (GeneTex, https://www.genetex.com) primary antibody. We blocked slide runs by group to account for potential differences between runs and scored as previously described (Appendix 1) (*23*).

Statistical analysis

We performed all statistical analyses using GraphPad Prism 8.1.2 software (https://www.graphpad.com). We used a Kruskal-Wallis test with Dunn correction for multiple comparisons to compare the weighted macroscopic lung lesion score, microscopic pneumonia score, microscopic tracheitis score, lung IHC score of conducting airways, lung IHC score of nonconducting airways, cumulative lung IHC scores, and tracheal IHC score of virus inoculated groups by dpi. We compared the BALF qRT-PCR Ct values of positive samples using an ordinary 1-way ANOVA with a Šídák multiple comparisons test. We considered an adjusted p value of <0.05 significant in each analysis.

Results

Isolate Replication

All isolates replicated in the lungs of most inoculated pigs, although no overt clinical signs were observed (Figure 2; Appendix 1 Table 1). We detected viral RNA in BALF from 3 of the 5 inoculated pigs necropsied at both 3 and 5 dpi in the A/turkey/MN/22

group, from all inoculated pigs necropsied at both 3 and 5 dpi in the A/bald eagle/FL/22 group, 4 of the 5 inoculated pigs necropsied at both 3 and 5 dpi in the A/raccoon/WA/22 group, and all inoculated pigs necropsied at 3 dpi and 4 inoculated pigs at 5 dpi in the A/redfox/MI/22 group. The lowest group mean Ct value (23.22) was observed in the A/bald eagle/FL/22 group at 5 dpi, followed by the A/raccoon/WA/22 group at 3 dpi (Ct value 26.05) and A/redfox/MI/22 group at 5 dpi (Ct value 26.14). The lowest individual Ct value (18.16) was seen in the A/raccoon/WA/22 group at 3 dpi. We found a significant difference in mean Ct values between the A/bald eagle/FL/22 and A/turkey/MN/22 groups and the A/bald eagle/FL/22 and A/raccoon/WA/22 groups at 5 dpi ($p<0.05$) (Figure 2). We did not detect viral RNA in BALF samples from control pigs.

Macroscopic and Microscopic Lesions

Macroscopic lung lesions consistent with IAV infection developed in pigs in each of the virus-inoculated groups. Macroscopic lesions consisted of multifocal-to-locally extensive predominately cranioventral red-to-purple pulmonary consolidation (Figure 3, panels A–D). Averaging the weighted macroscopic lung lesion score at 3 and 5 dpi by group showed that the A/bald eagle/FL/22 and A/redfox/MI/22 strains caused the highest lesion scores (Figure 4). A significant difference was found between groups necropsied at 5 dpi ($p<0.05$); however, no significant difference was found in the ad hoc comparisons with only the weighted macroscopic lung lesion score of the A/bald eagle/FL/22 group compared, and the A/turkey/MN/22 at 5 dpi neared significance ($p = 0.055$).

Microscopic lung lesions consistent with IAV infection developed in inoculated pigs in each of the virus-inoculated groups; however, the number of pigs with consistent lesions and the severity of lesions varied by group. A/turkey/MN/22 caused little to no microscopic lesions; lesions consistent with IAV infection developed in only 1 of 10 inoculated pigs (Figure 5, panel A). In contrast, lung lesions consistent with IAV infection developed in most pigs in the A/bald eagle/FL/22 group (7 of 10) (Figure 5, panel B). In both the A/raccoon/WA/22 and A/redfox/MI/22 groups, lesions consistent with IAV infection

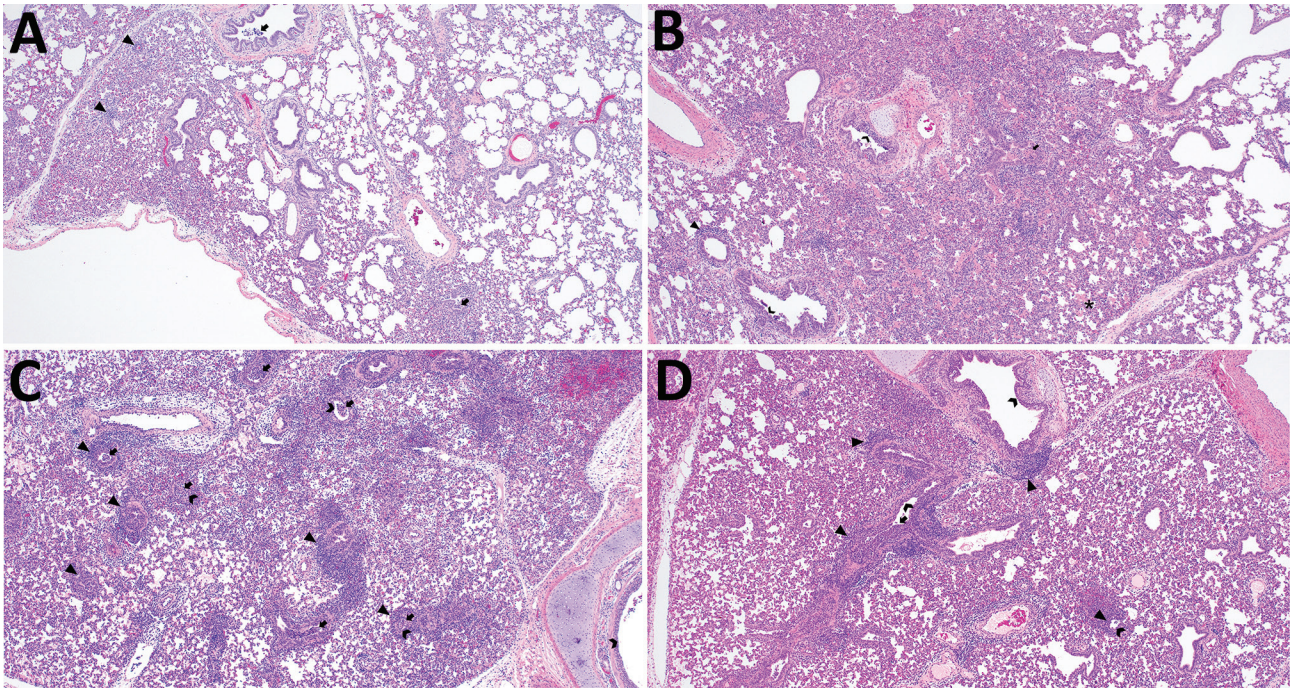

Figure 5. Microscopic lung lesions of swine infected with highly pathogenic avian influenza A(H5N1) belonging to the goose/Guangdong 2.3.4.4b hemagglutinin phylogenetic clade. A) Perivascular mononuclear inflammatory infiltrate (arrowheads) and suppurative bronchiolitis (arrows) in the lung of pig 777 infected with A/turkey/MN/22 necropsied at 3 days postinoculation (dpi). B) Peribronchiolar mononuclear inflammatory infiltrate (arrowhead), suppurative bronchiolitis (arrow), necrotizing bronchiolitis and bronchitis (chevrons), and alveolar luminal accumulation of cellular debris (asterisk) in the lung of pig 796 infected with A/bald eagle/FL/22 necropsied at 5 dpi. C) Peribronchiolar mononuclear inflammatory infiltrate (arrowheads), suppurative bronchiolitis (arrows), and necrotizing bronchiolitis and bronchitis (chevrons) in the lung of pig 58 infected with A/raccoon/WA/22 necropsied at 3 dpi. D) Peribronchiolar and peribronchial mononuclear inflammatory infiltrate (arrowheads), suppurative bronchiolitis (arrow), and necrotizing bronchiolitis and bronchitis (chevrons) in the lung of pig 78 infected with A/redfox/MI/22 necropsied at 3 dpi. Hematoxylin & eosin stain; original magnification ×40.

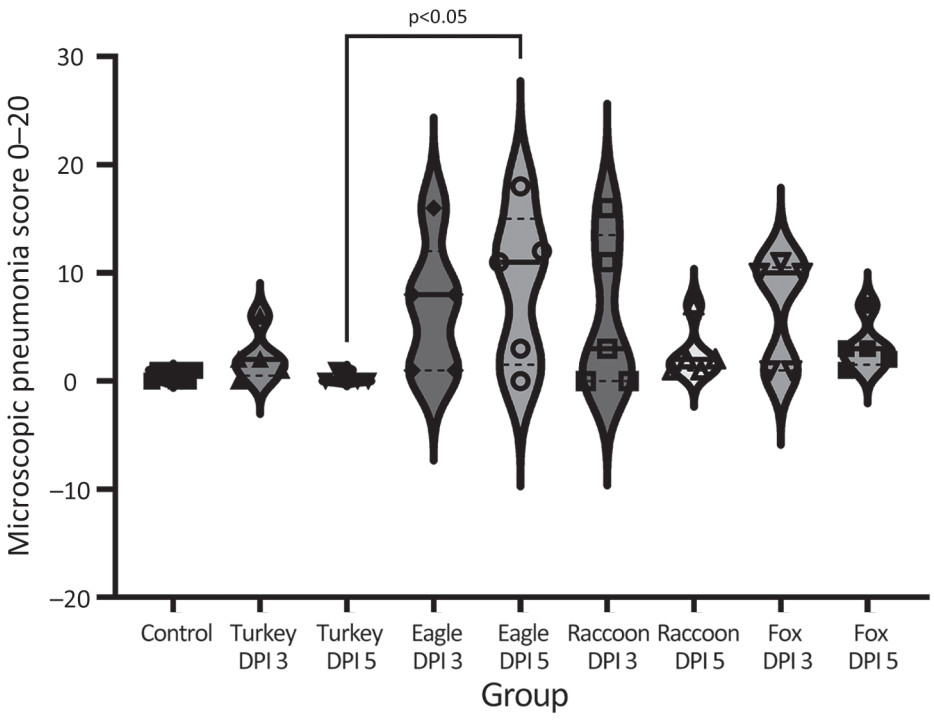

Figure 6. Violin plots of microscopic pneumonia scores, by virus strain and dpi, of swine infected with highly pathogenic avian influenza A(H5N1) virus belonging to the goose/Guangdong 2.3.4.4b hemagglutinin phylogenetic clade. Lesion severity varied by group, with the most severe lesions being observed in the A/bald eagle/FL/22 and A/red fox/MI/22 groups. Solid lines within plots indicate medians, dashed lines indicate quartiles, and symbols indicate individual pig values. dpi, days postinoculation; eagle 3 dpi, A/bald eagle/FL/22 necropsied at 3 dpi; eagle 5 dpi, A/bald eagle/FL/22 necropsied at 5 dpi; fox 3 dpi, A/redfox/MI/22 necropsied at 3 dpi; fox 5 dpi, A/redfox/MI/22 necropsied at 5 dpi; raccoon 3 dpi, A/raccoon/WA/22 necropsied at 3 dpi; raccoon 5 dpi, A/raccoon/WA/22 necropsied at 5 dpi; turkey 3 dpi, A/turkey/MN/22 necropsied at 3 dpi; turkey 5 dpi, A/turkey/MN/22 necropsied at 5 dpi.

developed in 4 of 10 inoculated pigs (Figure 5, panels C, D). A significant difference was found between the microscopic pneumonia score when comparing the A/turkey/MN/22 DPI 5 group and the A/bald eagle/FL/22 DPI 5 group ($p<0.05$) (Figure 6). Microscopic tracheitis scores were not statistically different between the virus inoculated groups (Appendix 1 Figure 1).

Alveolitis and Antigen Labeling

Divergent pathogenesis between HPAI strains was further evidenced by the extent of alveolitis and differential distribution and abundance of NP antigen by IHC. We did not detect HPAI NP antigen in any lung section from the A/turkey/MN/22 group but did detect HPAI NP antigen in the trachea of 2 pigs from this group. In contrast, we detected HPAI NP antigen in the trachea (8 of 10) and lung (7 of 10) in pigs in the A/bald eagle/FL/22 group. We also detected antigen in the respiratory epithelium of conducting airways, macrophages, pneumocytes, alveolar luminal debris, and, rarely, endothelial cells of pigs inoculated with A/bald eagle/FL/22 (Figure 7, panels A–C). In addition, the degree of alveolitis characterized by extensive widening of alveolar septa because of a mononuclear inflammatory infiltrate and luminal accumulation of edema and cellular debris, a change not typical of swine-adapted IAV, was most prominent in the A/bald eagle/FL/22 group (Figure 7, panels A, B).

We detected HPAI NP antigen in the trachea (6 of 10) or lung (2 of 10) of pigs from the A/raccoon/WA/22 group and trachea (7 of 10) or lung (5 of 10) of pigs in the A/redfox/MI/22 group. However, the distribution of antigen in those 2 groups varied compared to the A/bald eagle/FL/22 group. NP antigen was less commonly observed in macrophages, pneumocytes, and alveolar luminal debris and not observed in endothelial cells (Figure 7, panels D, E). We observed significant differences among the conducting airway (Figure 8, panel A), nonconducting airway (Figure 8, panel B), and cumulative lung IHC scores (Appendix 1 Figure 2) of the A/bald eagle/FL/22 5 dpi group and both the A/turkey/MN/22 group and A/raccoon/WA/22 5 dpi groups ($p<0.05$). We observed no significant difference for tracheal IHC score between the virus-inoculated groups (Appendix 1 Figure 3). We did not detect NP antigen in any samples from control pigs.

Mammalian Isolates

Neither A/turkey/MN/22 nor A/bald eagle/FL/22 replicated to detectable levels in the nasal cavity of inoculated pigs (0 of 15 per strain) or transmitted on the basis of seroconversion or detection of viral RNA in nasal swab samples from direct-contact pigs (0 of 5

per strain) (Table 2). In contrast, we detected A/raccoon/WA/22 in the nasal cavity of inoculated pigs (4 of 15) and transmitted to contacts (2 of 5). Similarly, we detected A/redfox/MI/22 in the nasal cavity of inoculated pigs (5 of 15) and transmitted to a single contact (Table 3). We did not detect viral RNA in any nasal swab samples from control pigs.

We identified within-host variants in PCR-positive samples across the genome for the 4 strains during infection and after transmission that were present in ≥1% of sequencing reads (Appendix 1 Table 2). Most single-nucleotide variants were present at low frequencies (Appendix 2, https://wwwnc.cdc.gov/EID/article/30/4/23-1141-App2.xlsx). Of the polymorphic amino acid sites, 41 nonsynonymous mutations occurred at sites associated with functional changes, including PB2 E627K detected as a minor variant (4.95%) in A/turkey/MN/22 at 5 dpi in a single sample

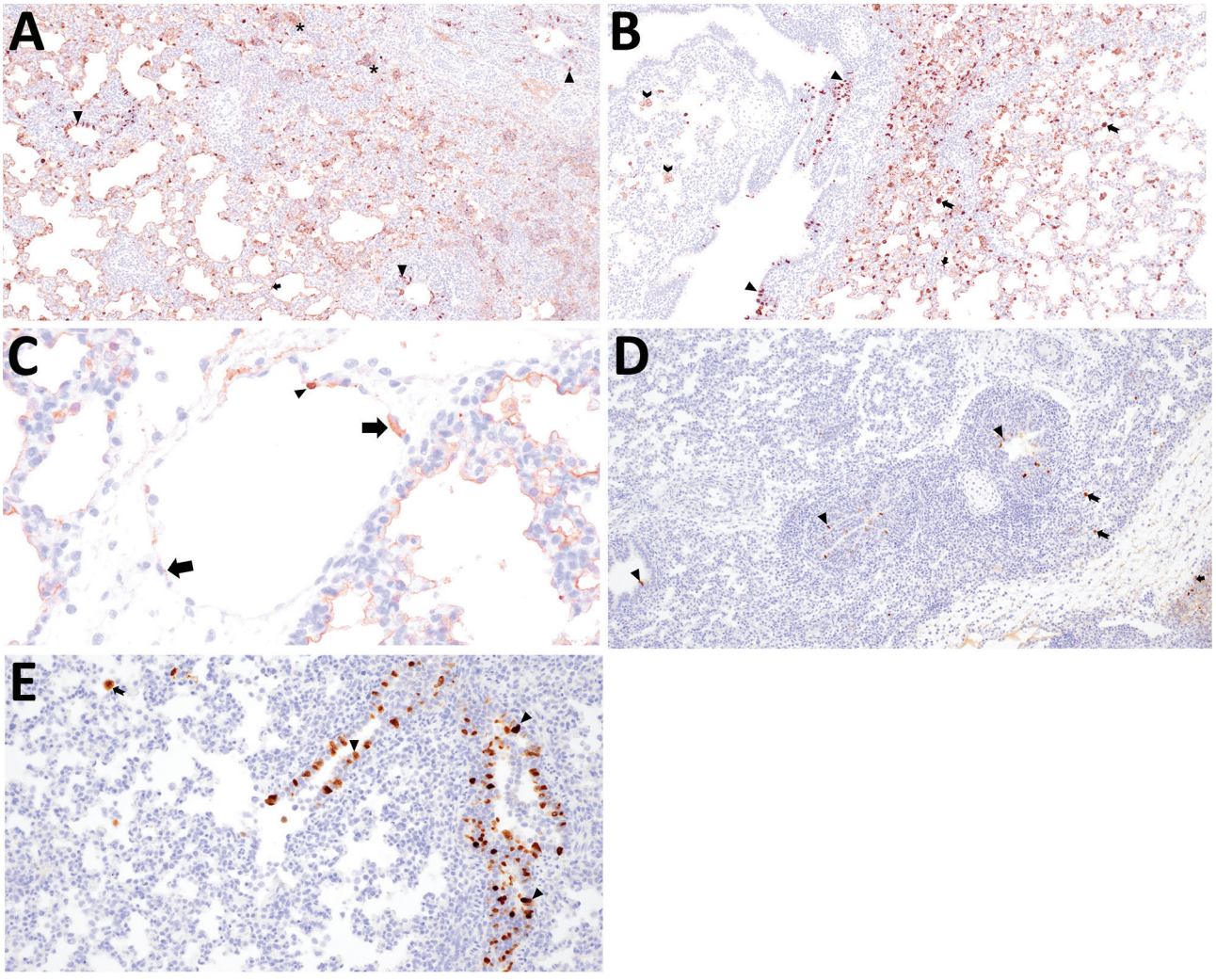

Figure 7. Immunohistochemical detection of influenza A virus nucleoprotein antigen in swine infected with H5N1 highly pathogenic avian influenza belonging to the goose/Guangdong 2.3.4.4b hemagglutinin phylogenetic clade. A) Extensive labeling of pneumocytes lining alveolar septa (arrows) and respiratory epithelium lining bronchioles (arrowheads) in the lung of pig 794 infected with A/bald eagle/FL/22 necropsied at 3 days postinoculation (dpi). Hematoxylin & eosin stain; original magnification ×40. B) Extensive labeling of pneumocytes lining alveolar septa (arrow), respiratory epithelium lining a bronchus (arrowheads), cell membrane of alveolar macrophages (chevron), and within the cytoplasm and nucleus of alveolar macrophages consistent with viral replication (notched arrow) in the lung of pig 798 infected with A/bald eagle/FL/22 necropsied on 5 dpi. Hematoxylin & eosin stain; original magnification ×40. C) Labeling in the cytoplasm (arrows) and nucleus (arrowhead) of endothelial cells in the lung of pig 791 infected with A/bald eagle/FL/22 necropsied on 3 dpi. Hematoxylin & eosin stain; original magnification ×200. D) Labeling of respiratory epithelium lining a bronchus (arrowheads), within the cytoplasm and nucleus of alveolar macrophages consistent with viral replication (notched arrow), rarely pneumocytes (arrow), in the lung of pig 58 infected with A/raccoon/WA/22 necropsied on 3 dpi. Hematoxylin & eosin stain; original magnification ×40. E) Abundant labeling of respiratory epithelium lining a bronchiole (arrowheads) and within the cytoplasm and nucleus of alveolar macrophages consistent with viral replication (notched arrow) in the lung of pig 78 infected with A/redfox/MI/22 necropsied on 3 dpi. Hematoxylin & eosin stain; original magnification ×100.

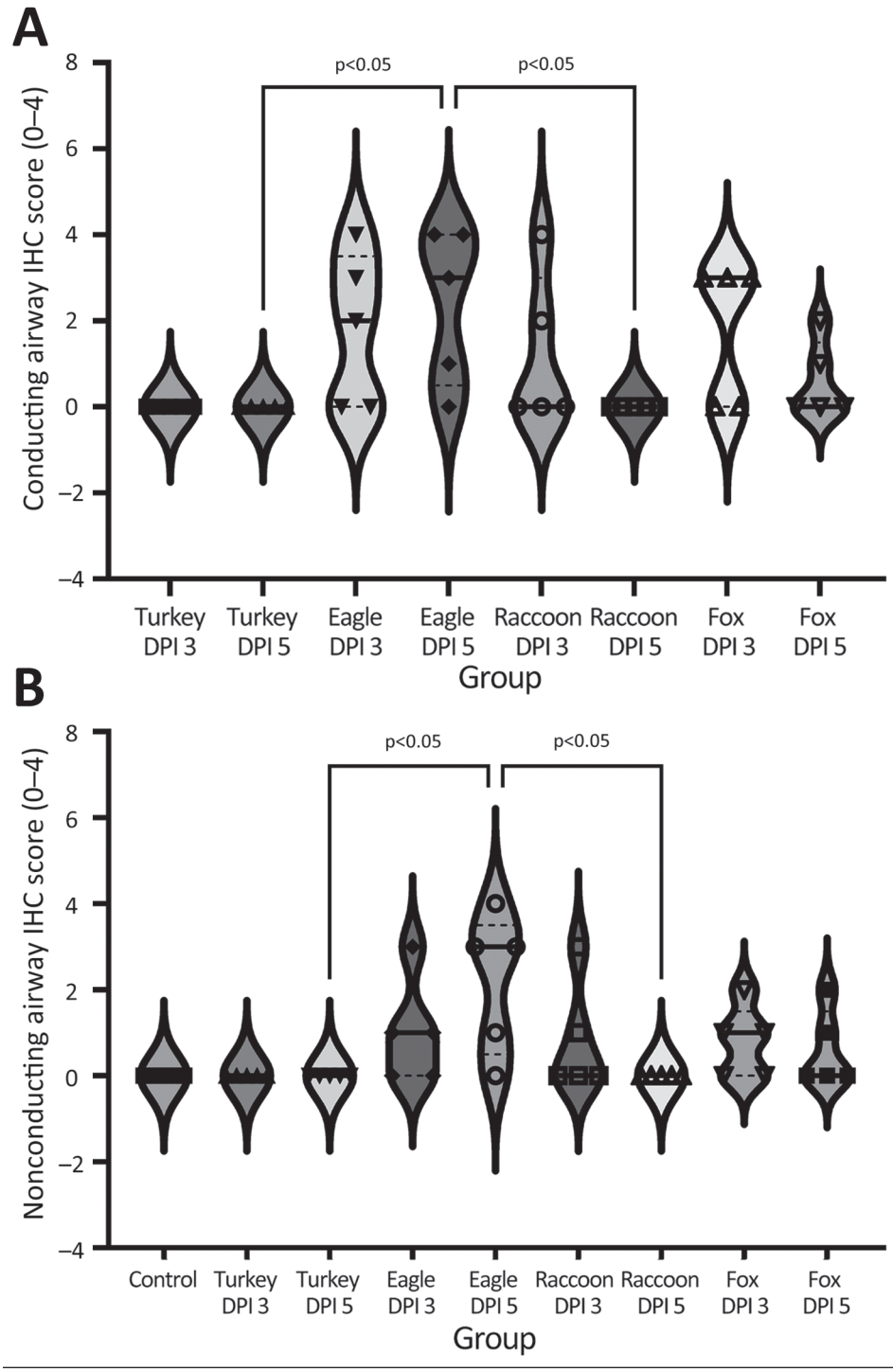

Figure 8. Violin plots of airway conducting IHC scores, by virus strain and dpi, of swine infected with highly pathogenic avian influenza A(H5N1) virus belonging to the goose/Guangdong 2.3.4.4b hemagglutinin phylogenetic clade. A) Lung conducting airway immunohistochemical scores. Influenza A virus (IAV) nucleoprotein (NP) antigen detection varied by group with the most extensive labeling (the number of positive pigs) being observed in the A/bald eagle/FL/22 and A/red fox/MI/22 groups. B) Lung nonconducting airway immunohistochemical scores. IAV NP antigen detection varied by group with the most extensive labeling being observed in the A/bald eagle/FL/22. Solid lines within plots indicate medians, dashed lines indicate quartiles, and symbols indicate individual pig values. dpi, days postinoculation; eagle 3 dpi, A/bald eagle/FL/22 necropsied at 3 dpi; eagle 5 dpi, A/bald eagle/FL/22 necropsied at 5 dpi; fox 3 dpi, A/redfox/MI/22 necropsied at 3 dpi; fox 5 dpi, A/redfox/MI/22 necropsied at 5 dpi; IHC, immunohistochemistry; raccoon 3 dpi, A/raccoon/WA/22 necropsied at 3 dpi; raccoon 5 dpi, A/raccoon/WA/22 necropsied at 5 dpi; turkey 3 dpi, A/turkey/MN/22 necropsied at 3 dpi; turkey 5 dpi, A/turkey/MN/22 necropsied at 5 dpi.

(Appendix 2). We also detected Polymorphisms at low levels in the A/bald eagle/FL/22 and A/turkey/MN/22 HA gene at position 239 (R239H and R239C). We also detected HA mutations associated with receptor binding affinity at low levels in single samples in A/redfox/MI/22 (S110N, P139L, L513S) and A/raccoon/WA/22 (S110N, M404V, E267K).

We calculated synonymous (π_S) and nonsynonymous (π_N) polymorphisms to assess selection; we considered π_N/π_S <1 suggestive of purifying selection and π_N/π_S >1 suggestive of positive selection. When we combined the diversity estimates across genes, all strains exhibited π_N/π_S <1 (A/turkey/MN/22 π_N/π_S = 0.36; A/bald eagle/FL/22 π_N/π_S = 0.40; A/redfox/

MI/22 π_N/π_S = 0.50; A/raccoon/WA/22 π_N/π_S = 0.74), suggesting that the within-host populations tended to exhibit weak purifying selection.

Discussion

We conducted a pathogenesis and transmission study to understand the susceptibility of swine to 3 genotypes of HPAI H5N1 belonging to the goose/Guangdong 2.3.4.4b HA phylogenetic clade detected within the United States. Our data demonstrated that pigs are susceptible to infection. All 4 HPAI isolates that were evaluated replicated in the lungs of pigs. In comparison to an H1N1 swine-adapted virus, the qRT-PCR Ct values in BALF of the 4 HPAI strains were lower (≈3–8 Ct), except for the A/bald eagle/FL/22 (genotype B1.1) 5 dpi group (Appendix 1 Table 3) (*24*). Replication in the nasal cavity and transmission occurred only in the A/raccoon/WA/22 (genotype B2.1) and A/redfox/MI/22 (genotype B3.2) groups containing the mammalian adaptation mutation E627K in the PB2 gene. However, the number of pigs with qRT-PCR–positive nasal swabs was considerably lower than for the swine-adapted virus; the approximate viral load was lower (≈4–6 Ct), and detection was later (1 dpi vs. 5 or 7 dpi) (Appendix 1 Table 4) (*24*). Pig 61 (relatively early detection) might have infected inoculated cohorts, and transmission to contacts at later points not captured in our study design might have occurred. The finding of replication of HPAI H5NX clade 2.3.4.4x in the lung of pigs in an experimental model has been shown, but demonstrating replication in the nasal cavity and transmission to contact pigs is novel (*25*,*26*). In addition, a recent study deemed pigs to be highly resistant to clade 2.3.4.4b infection, illustrating the need for continued assessment of genetically diverse viruses with variable phenotypes in pigs (*27*).

The effects of HPAI viruses can range from asymptomatic infections to severe disease in mammals (*28*–*31*). Multiple viral proteins contribute to the pathogenicity and transmissibility of HPAI, and a combination of adaptive mutations and reassortment are likely necessary for efficient mammal transmission (*32*). Both mammal isolates evaluated in this study contained the PB2 E627K mutation, were detected in the noses of inoculated pigs, and transmitted to ≥1 contact pig. The PB2 gene of all human seasonal viruses of the 20th century contain K627, whereas most clade 2.3.4.4b viruses detected in birds in 2022–2023 contain E627, supporting the role of that mutation in mammalian adaptation (*1*,*17*). Although we did not fully evaluate the direct effects of the E627K mutation in swine, the shedding and transmission profile shown for the 2 mammal isolates in this study indicate this adaptive mutation might have increased viral fitness through enhanced polymerase activity to enable transmission in an otherwise less susceptible host.

Whether different internal gene constellations or other genotypic differences between A/bald eagle/FL/22 (North American PB2, PB1, and NP) and A/turkey/MN/22 (North American PB2 and NP; genotype 2.1) are responsible for the pathogenic differences of those isolates in pigs is unknown. The number of North American gene segments in reassorted HPAI H5N1 clade 2.3.4.4b avian isolates and disease severity in mammals was suggested to have a positive correlation in ferret and mice models (*11*). Although we did not observe evidence of shedding or transmission, both avian isolates replicated in the lung, which is concerning because of potential reassortment with endemic swine viruses.

Viral populations were dominated by low-frequency (<5%) variation that appeared to be shaped by purifying selection. We detected a subset of mutations associated with human receptor binding and specificity (HA S110N, P139L, R239C/H, E267K, L513S) and mammalian replication (PB2 E627K). However, the detected mutations remained at low frequency, and those present early were not transmitted, did not persist, and were not consistently detected across animals. Those data are in accordance with previous studies documenting within-host evolution of H5N1 in poultry (*33*–*35*). Consequently, though adaptive mutations might occur during H5N1 infection in pigs, because of the short infection time and presence of purifying selection (π_N/π_S <1), the evolutionary potential of the strains in this study appears

Table 2. Replication and transmission data in study of divergent pathogenesis and transmission of highly pathogenic avian influenza A(H5N1) in swine*

	Inoculated pigs				Contact pigs	
Strain	NS PCR-positive	BALF PCR-positive, 3 dpi	BALF PCR-positive, 5 dpi	Seroconversion	NS PCR-positive	Seroconversion
A/turkey/MN/22	0/15	3/5	3/5	2/5	0/5	0/5
A/bald eagle/FL/22	0/15	5/5	5/5	3/5	0/5	0/5
A/raccoon/WA/22	4/15	4/5	5/5	5/5	2/5	1/5
A/red fox/MI/22	5/15	5/5	4/5	5/5	0/5	1/5

*Nasal swab samples were taken on 0, 1, 3, 5, and 7 dpi or dpc. BALF was collected at 3 and 5 dpi. Influenza A virus qRT-PCR. Seroconversion results of inoculated pigs are only on surviving pigs at ≈2 weeks dpi or dpc. BALF, bronchoalveolar lavage fluid; dpc, days postcontact; dpi, days postinoculation; NS, nasal swab; qRT-PCR, quantitative reverse transcription PCR.

limited, and the functional effects for the documented mutations require additional study.

The HA proteins of HPAI H5N1 2.3.4.4b virus preferentially bind to α2,3-linked sialic acids on the host cell (*11*), which are at low abundance in the porcine upper respiratory system (*32*). The low abundance of α2,3-linked sialic acids on epithelial cells in the pigs' nasal cavities might explain why HPAI avian isolates did not transmit. The quantity of α2,3-linked sialic acids is relatively higher in the lungs of pigs and humans and localized to pneumocytes and nonciliated bronchiolar cells (*36*–*39*). That distribution is consistent with the extent and distribution of IHC IAV NP labeling in the lung of pigs inoculated with A/bald eagle/FL/22; we noted prominent alveolitis in those pigs, in contrast to those inoculated with either A/raccoon/WA/22 or A/redfox/MI/22.

Table 3. Ct values for nasal swab samples tested for influenza A virus by qRT-PCR by pig and days postinoculation for A/raccoon/WA/22 and A/redfox/MI/22 strains

	Days postinoculation or postcontact				
Pig ID	0	1	3	5	7
A/raccoon/WA/22					
56	ND	ND	ND	NA	NA
57	ND	ND	ND	NA	NA
58	ND	ND	ND	NA	NA
59	ND	ND	ND	NA	NA
60	ND	ND	ND	NA	NA
61	ND	33.0	34.7	33.2	NA
62	ND	ND	ND	ND	NA
63	ND	ND	ND	38.8	NA
64	ND	ND	ND	ND	NA
65	ND	ND	ND	32.1	NA
66	ND	ND	ND	ND	ND
67	ND	ND	ND	ND	29.5
68	ND	ND	ND	ND	ND
69	ND	36.5	ND	36.9	35.1
70	ND	ND	ND	ND	ND
71	ND	ND	ND	ND	38.1
72	ND	ND	ND	ND	32.5
73	ND	ND	ND	ND	35.0
74	ND	ND	ND	ND	ND
75	ND	ND	ND	ND	ND
A/redfox/MI/22					
76	ND	ND	ND	NA	NA
77	ND	ND	ND	NA	NA
78	ND	ND	ND	NA	NA
79	ND	ND	ND	NA	NA
80	ND	ND	ND	NA	NA
81	ND	ND	ND	ND	NA
82	ND	ND	ND	ND	NA
83	ND	ND	ND	ND	NA
84	ND	ND	ND	ND	NA
85	ND	ND	34.8	ND	NA
86	ND	ND	28.1	39.2	37.1
87	ND	ND	ND	ND	37.9
88	ND	ND	ND	36.0	ND
89	ND	ND	ND	35.4	ND
90	ND	ND	ND	38.9	ND
91	ND	ND	ND	ND	ND
92	ND	ND	ND	ND	ND
93	ND	ND	ND	ND	ND
94	ND	ND	ND	ND	ND
95	ND	ND	ND	ND	ND

*Ct value of <38.0 indicates a positive sample, 38–40 indicates suspect sample, and ND indicates negative sample. Pigs numbered 71–75 and 91–95 are contact pigs. Ct, cycle threshold; ID, identification; NA, not available (pig previously euthanized as part of study design); ND, not detected; qRT-PCR, quantitative reverse transcription PCR.

Interspecies spillovers commonly result in dead-end infections because the virus likely requires multiple transmission events to acquire the necessary adaptive mutations (*40*). The probability of a virus acquiring a complete set of adaptive mutations in a single immunocompetent host with onward transmission is extremely low (*34*). However, continued circulation of HPAI strains that have already adapted within various mammalian species makes that possibility more likely (*1*,*34*). On-farm transmission among pigs in Indonesia of an HPAI H5N1 and identification of a purified clone with the ability to recognize α2,6 sialic acid receptors were reported (*3*). More recently, serologic evidence of infection of domestic pigs with clade 2.3.4.4b was reported (*41*). In addition, because reassortment occurred with the past 4 influenza pandemics, the propensity for reassortment in swine may increase the risk for H5N1 adaptation toward humans, particularly with the maintenance of 2009 pandemic H1N1 human seasonal virus genes in pigs (*42*). Although infrequent, incursion of LPAI into commercial swine herds in North America occurs periodically, yet the sources of incursion often remain unknown (*43*–*45*). Increased viral fitness characterized by transmission of LPAI strains after reassortment with swine-adapted IAV in pigs was demonstrated both in commercial swine herds and experimentally (*43*,*46*).

The genetic attributes that resulted in the continued circulation of the HPAI H5N1 2.3.4.4b lineage are not well understood. Repeated spillover and spillback events resulted in genotypically and phenotypically diverse reassortant viruses, some of which caused neurologic disease in mammals, a manifestation not observed in pigs (*47*). However, detection of NP antigen in endothelial cells of pigs infected with A/bald eagle/FL/22 suggests this strain might spread systemically.

The risk for reassortment of the HPAI H5N1 2.3.4.4b lineage with endemic swine IAV is a consideration on the basis of the susceptibility to this lineage demonstrated in our study, the prevalence of IAV infection and comorbidities in swine herds, and animal husbandry practices (*48*,*49*). However, the risk for incursion is likely lower in confinement operations with industry standard biosecurity than for backyard or feral pigs. Birdproofing feed and facilities, avoiding the use of untreated water, and restricting peridomestic scavenger mammals from premises are measures to increase biosecurity against HPAI H5N1 clade 2.3.4.4b virus incursion into swine herds.

Acknowledgments

We thank Nicholas Otis for his technical assistance; Randy Leon, Adam Hartfiel, Alyssa Dannen, Justin Miller, Jason Huegel, Derek Vermeer, Rebecca Cox, Kolby Stallman, and Jonathan Gardner for assistance with animal care and sample collection; and Judith Stasko and Adrienne Shircliff for preparation of histologic sections. We also gratefully acknowledge all data contributors (i.e., the authors and their originating laboratories responsible for obtaining the specimens, and their submitting laboratories for generating the genetic sequence and metadata and sharing via the GISAID Initiative [https://www.gisaid.org], on which components of this research is based). In addition, we are grateful to colleagues at the USDA ARS Southeast Poultry Research Laboratory for their contribution of the H5 2.3.4.4 assay.

This project was funded in part with Federal funds from the National Institute of Allergy and Infectious Diseases, National Institutes of Health, Department of Health and Human Services (contract no. 75N93021C00015) and the U.S. Department of Agriculture (USDA) Agricultural Research Service (contract no. 5030-32000-231-000-D). Mention of trade names or commercial products in this article is solely for the purpose of providing specific information and does not imply recommendation or endorsement by the NIH or USDA. Funding sources had no role in experimental design, data collection/analysis/interpretation, preparation of the manuscript, or decision to publish. USDA is an equal opportunity provider and employer.

About the Author

Dr. Arruda is a research veterinary medical officer and veterinary pathologist at the National Animal Disease Center. Her research focuses on intervention strategies to prevent and respond to influenza A virus infections in swine.

References

1. Long JS, Mistry B, Haslam SM, Barclay WS. Host and viral determinants of influenza A virus species specificity. Nat Rev Microbiol. 2019;17:67–81. https://doi.org/10.1038/s41579-018-0115-z
2. Belser JA, Tumpey TM. H5N1 pathogenesis studies in mammalian models. Virus Res. 2013;178:168–85. https://doi.org/10.1016/j.virusres.2013.02.003
3. Nidom CA, Takano R, Yamada S, Sakai-Tagawa Y, Daulay S, Aswadi D, et al. Influenza A (H5N1) viruses from pigs, Indonesia. Emerg Infect Dis. 2010;16:1515–23. https://doi.org/10.3201/eid1610.100508
4. Centers for Disease Control and Prevention. Technical report: highly pathogenic avian influenza A(H5N1) viruses [cited 2023 Mar 24]. https://www.cdc.gov/flu/avianflu/spotlights/2022-2023/h5n1-technical-report.htm#human-cases
5. Animal and Plant Health Inspection Office. 2022–2024 detections of highly pathogenic avian influenza in mammals [cited 2023 Dec 15]. https://www.aphis.usda.gov/aphis/ourfocus/animalhealth/animal-disease-information/avian/avian-influenza/hpai-2022/2022-hpai-mammals
6. Animal and Plant Health Inspection Office. 2022–20243 confirmations of highly pathogenic avian influenza in commercial and backyard flocks [cited 2023 Mar 24]. https://www.aphis.usda.gov/aphis/ourfocus/animalhealth/animal-disease-information/avian/avian-influenza/hpai-2022/2022-hpai-commercial-backyard-flocks
7. Lee DH, Criado MF, Swayne DE. Pathobiological origins and evolutionary history of highly pathogenic avian influenza viruses. Cold Spring Harb Perspect Med. 2021;11:a038679. https://doi.org/10.1101/cshperspect.a038679
8. Lee DH, Bertran K, Kwon JH, Swayne DE. Evolution, global spread, and pathogenicity of highly pathogenic avian influenza H5Nx clade 2.3.4.4. J Vet Sci. 2017;18(S1):269–80. https://doi.org/10.4142/jvs.2017.18.S1.269
9. Pohlmann A, King J, Fusaro A, Zecchin B, Banyard AC, Brown IH, et al. Has epizootic become enzootic? Evidence for a fundamental change in the infection dynamics of highly pathogenic avian influenza in Europe, 2021. MBio. 2022;13:e0060922. https://doi.org/10.1128/mbio.00609-22
10. Bevins SN, Shriner SA, Cumbee JC Jr, Dilione KE, Douglass KE, Ellis JW, et al. Intercontinental movement of highly pathogenic avian influenza A(H5N1) clade 2.3.4.4 virus to the United States, 2021. Emerg Infect Dis. 2022;28:1006–11. https://doi.org/10.3201/eid2805.220318
11. Kandeil A, Patton C, Jones JC, Jeevan T, Harrington WN, Trifkovic S, et al. Rapid evolution of A(H5N1) influenza viruses after intercontinental spread to North America. Nat Commun. 2023;14:3082. https://doi.org/10.1038/s41467-023-38415-7
12. Youk S, Torchetti MK, Lantz K, Lenoch JB, Killian ML, Leyson C, et al. H5N1 highly pathogenic avian influenza clade 2.3.4.4b in wild and domestic birds: introductions into the United States and reassortments, December 2021–April 2022. Virology. 2023;587:109860.
13. Sun H, Pu J, Wei Y, Sun Y, Hu J, Liu L, et al. Highly pathogenic avian influenza H5N6 viruses exhibit enhanced affinity for human type sialic acid receptor and in-contact transmission in model ferrets. J Virol. 2016;90:6235–43. https://doi.org/10.1128/JVI.00127-16
14. Yamaji R, Saad MD, Davis CT, Swayne DE, Wang D, Wong FYK, et al. Pandemic potential of highly pathogenic avian influenza clade 2.3.4.4 A(H5) viruses. Rev Med Virol. 2020;30:e2099. https://doi.org/10.1002/rmv.2099
15. Pulit-Penaloza JA, Brock N, Pappas C, Sun X, Belser JA, Zeng H, et al. Characterization of highly pathogenic avian influenza H5Nx viruses in the ferret model. Sci Rep. 2020;10:12700. https://doi.org/10.1038/s41598-020-69535-5
16. Zhao Z, Guo Z, Zhang C, Liu L, Chen L, Zhang C, et al. Avian influenza H5N6 viruses exhibit differing pathogenicities and transmissibilities in mammals. Sci Rep. 2017;7:16280. https://doi.org/10.1038/s41598-017-16139-1
17. Adlhoch C, Fusaro A, Gonzales JL, Kuiken T, Marangon S, Mirinaviciute G, et al.; European Food Safety Authority; European Centre for Disease Prevention and Control; European Union Reference Laboratory for Avian Influenza. Avian influenza overview December 2022–March 2023. EFSA J. 2023;21:e07917.
18. Centers for Disease Control and Prevention. Human infection with highly pathogenic avian influenza A(H5N1) virus in Chile [cited 2023 May 2]. https://www.cdc.gov/flu/avianflu/spotlights/2022-2023/chile-first-case-h5n1-addendum.htm

19. Vincent AL, Lager KM, Ma W, Lekcharoensuk P, Gramer MR, Loiacono C, et al. Evaluation of hemagglutinin subtype 1 swine influenza viruses from the United States. Vet Microbiol. 2006;118:212–22. https://doi.org/10.1016/j.vetmic.2006.07.017
20. Youk S, Torchetti MK, Lantz K, Lenoch JB, Killian ML, Leyson C, et al. H5N1 highly pathogenic avian influenza clade 2.3.4.4b in wild and domestic birds: introductions into the United States and reassortments, December 2021–April 2022. Virology. 2023;587:109860. https://doi.org/10.1016/j.virol.2023.109860
21. Zhang Y, Aevermann BD, Anderson TK, Burke DF, Dauphin G, Gu Z, et al. Influenza Research Database: an integrated bioinformatics resource for influenza virus research. Nucleic Acids Res. 2017;45(D1):D466–74. https://doi.org/10.1093/nar/gkw857
22. Nelson CW, Moncla LH, Hughes AL. SNPGenie: estimating evolutionary parameters to detect natural selection using pooled next-generation sequencing data. Bioinformatics. 2015;31:3709–11. https://doi.org/10.1093/bioinformatics/btv449
23. Gauger PC, Vincent AL, Loving CL, Henningson JN, Lager KM, Janke BH, et al. Kinetics of lung lesion development and pro-inflammatory cytokine response in pigs with vaccine-associated enhanced respiratory disease induced by challenge with pandemic (2009) A/H1N1 influenza virus. Vet Pathol. 2012;49:900–12. https://doi.org/10.1177/0300985812439724
24. Arruda BL, Kanefsky RA, Hau S, Janzen GM, Anderson TK, Vincent Baker AL. Mucin 4 is a cellular biomarker of necrotizing bronchiolitis in influenza A virus infection. Microbes Infect. 2023;25:105169. https://doi.org/10.1016/j.micinf.2023.105169
25. Lipatov AS, Kwon YK, Sarmento LV, Lager KM, Spackman E, Suarez DL, et al. Domestic pigs have low susceptibility to H5N1 highly pathogenic avian influenza viruses. PLoS Pathog. 2008;4:e1000102. https://doi.org/10.1371/journal.ppat.1000102
26. Kaplan BS, Torchetti MK, Lager KM, Webby RJ, Vincent AL. Absence of clinical disease and contact transmission of HPAI H5NX clade 2.3.4.4 from North America in experimentally infected pigs. Influenza Other Respir Viruses. 2017;11:464–70. https://doi.org/10.1111/irv.12463
27. Graaf A, Piesche R, Sehl-Ewert J, Grund C, Pohlmann A, Beer M, et al. Low susceptibility of pigs against experimental infection with HPAI virus H5N1 clade 2.3.4.4b. Emerg Infect Dis. 2023;29:1492–5. https://doi.org/10.3201/eid2907.230296
28. Shin DL, Siebert U, Lakemeyer J, Grilo M, Pawliczka I, Wu NH, et al. Highly pathogenic avian influenza A(H5N8) virus in gray seals, Baltic Sea. Emerg Infect Dis. 2019;25:2295–8. https://doi.org/10.3201/eid2512.181472
29. Floyd T, Banyard AC, Lean FZX, Byrne AMP, Fullick E, Whittard E, et al. Encephalitis and death in wild mammals at a rehabilitation center after infection with highly pathogenic avian influenza A(H5N8) virus, United Kingdom. Emerg Infect Dis. 2021;27:2856–63. https://doi.org/10.3201/eid2711.211225
30. Postel A, King J, Kaiser FK, Kennedy J, Lombardo MS, Reineking W, et al. Infections with highly pathogenic avian influenza A virus (HPAIV) H5N8 in harbor seals at the German North Sea coast, 2021. Emerg Microbes Infect. 2022;11:725–9. https://doi.org/10.1080/22221751.2022.2043726
31. Rijks JM, Hesselink H, Lollinga P, Wesselman R, Prins P, Weesendorp E, et al. Highly pathogenic avian influenza A(H5N1) virus in wild red foxes, the Netherlands, 2021. Emerg Infect Dis. 2021;27:2960–2. https://doi.org/10.3201/eid2711.211281
32. Neumann G. H5N1 influenza virulence, pathogenicity and transmissibility: what do we know? Future Virol. 2015;10:971–80. https://doi.org/10.2217/fvl.15.62
33. Moncla LH, Bedford T, Dussart P, Horm SV, Rith S, Buchy P, et al. Quantifying within-host diversity of H5N1 influenza viruses in humans and poultry in Cambodia. PLoS Pathog. 2020;16:e1008191. https://doi.org/10.1371/journal.ppat.1008191
34. Russell CA, Fonville JM, Brown AE, Burke DF, Smith DL, James SL, et al. The potential for respiratory droplet-transmissible A/H5N1 influenza virus to evolve in a mammalian host. Science. 2012;336:1541–7. https://doi.org/10.1126/science.1222526
35. Bordes L, Vreman S, Heutink R, Roose M, Venema S, Pritz-Verschuren SBE, et al. Highly pathogenic avian influenza H5N1 virus infections in wild red foxes (Vulpes vulpes) show neurotropism and adaptive virus mutations. Microbiol Spectr. 2023;11:e0286722. https://doi.org/10.1128/spectrum.02867-22
36. Baum LG, Paulson JC. Sialyloligosaccharides of the respiratory epithelium in the selection of human influenza virus receptor specificity. Acta Histochem Suppl. 1990;40:35–8.
37. Nicholls JM, Chan MC, Chan WY, Wong HK, Cheung CY, Kwong DL, et al. Tropism of avian influenza A (H5N1) in the upper and lower respiratory tract. Nat Med. 2007;13:147–9. https://doi.org/10.1038/nm1529
38. Shinya K, Ebina M, Yamada S, Ono M, Kasai N, Kawaoka Y. Avian flu: influenza virus receptors in the human airway. Nature. 2006;440:435–6. https://doi.org/10.1038/440435a
39. Yao L, Korteweg C, Hsueh W, Gu J. Avian influenza receptor expression in H5N1-infected and noninfected human tissues. FASEB J. 2008;22:733–40. https://doi.org/10.1096/fj.06-7880com
40. Illingworth CJ. Fitness inference from short-read data: within-host evolution of a reassortant H5N1 influenza virus. Mol Biol Evol. 2015;32:3012–26. https://doi.org/10.1093/molbev/msv171
41. Rosone F, Bonfante F, Sala MG, Maniero S, Cersini A, Ricci I, et al. Seroconversion of a swine herd in a free-range rural multi-species farm against HPAI H5N1 2.3.4.4b clade virus. Microorganisms. 2023;11:1162. https://doi.org/10.3390/microorganisms11051162
42. Neumann G, Green MA, Macken CA. Evolution of highly pathogenic avian H5N1 influenza viruses and the emergence of dominant variants. J Gen Virol. 2010;91:1984–95. https://doi.org/10.1099/vir.0.020750-0
43. Ma W, Vincent AL, Gramer MR, Brockwell CB, Lager KM, Janke BH, et al. Identification of H2N3 influenza A viruses from swine in the United States. Proc Natl Acad Sci U S A. 2007;104:20949–54. https://doi.org/10.1073/pnas.0710286104
44. Karasin AI, Brown IH, Carman S, Olsen CW. Isolation and characterization of H4N6 avian influenza viruses from pigs with pneumonia in Canada. J Virol. 2000;74:9322–7. https://doi.org/10.1128/JVI.74.19.9322-9327.2000
45. Karasin AI, West K, Carman S, Olsen CW. Characterization of avian H3N3 and H1N1 influenza A viruses isolated from pigs in Canada. J Clin Microbiol. 2004;42:4349–54. https://doi.org/10.1128/JCM.42.9.4349-4354.2004
46. Abente EJ, Kitikoon P, Lager KM, Gauger PC, Anderson TK, Vincent AL. A highly pathogenic avian-derived influenza

virus H5N1 with 2009 pandemic H1N1 internal genes demonstrates increased replication and transmission in pigs. J Gen Virol. 2017;98:18–30. https://doi.org/10.1099/jgv.0.000678
47. Kandeil A, Patton C, Jones J, Jeevan T, Harrington W, Trifkovic S, et al. Rapid evolution of A(H5N1) influenza viruses after intercontinental spread to North America. Nat Commun. 2023;14:3082.
48. Zeller MA, Anderson TK, Walia RW, Vincent AL, Gauger PC. ISU FLUture: a veterinary diagnostic laboratory web-based platform to monitor the temporal genetic patterns of Influenza A virus in swine. BMC Bioinformatics. 2018;19:397. https://doi.org/10.1186/s12859-018-2408-7
49. Trevisan G, Schwartz KJ, Burrough ER, Arruda B, Derscheid RJ, Rahe MC, et al. Visualization and application of disease diagnosis codes for population health management using porcine diseases as a model. J Vet Diagn Invest. 2021;33:428–38.

Address for correspondence: Bailey Arruda, USDA National Animal Disease Center, 1920 Dayton Ave, Ames, IA 50010, USA; email: bailey.arruda@usda.gov

Article DOI: https://doi.org/10.3201/eid3004.231141

Divergent Pathogenesis and Transmission of Highly Pathogenic Avian Influenza A(H5N1) in Swine

Appendix

Additional Materials and Methods

Viruses

All strains retained the H5 and N1 from the 2.3.4.4b lineage. A/turkey/Minnesota/2022 contained North American LPAI PB2 and NP and is classified as a genotype B2.1. A/bald eagle/Florida/2022 contained North American LPAI PB2, PB1, and NP and is classified as a genotype B1.1 (*1*). Neither the A/turkey/Minnesota/2022 nor the A/bald eagle/Florida/2022 strains contained known mammalian adaptation mutations. A/raccoon/WA/22 contained North American LPAI PB2 and NP and is classified as a genotype B2.1. A/redfox/MI/22 contained North American LPAI PB1, PB2, NP, and NS and is classified as a genotype B3.2.

Swine pathogenesis and transmission study

Eighty-eight pigs were obtained from a herd free of influenza A virus (IAV), porcine reproductive and respiratory syndrome virus, and *Mycoplasma hyopneumoniae*. Prior to inoculation, pigs were confirmed seronegative to IAV by a blocking ELISA (IDEXX) and treated with tulathromycin (Zoetis) and ceftiofur crystalline free acid (Zoetis). Pigs were blocked by litter and randomly allocated using the Excel random function into a negative control group or a group of 20 (one group per virus strain), housed in individual containment rooms. Five naive contact pigs were comingled with each of the intranasally virus-inoculated groups at 2 days post-inoculation (DPI). Nasal swabs (Minitip FLOQSwabs) samples were collected on 0, 1, 3, 5, and 7 DPI from inoculated pigs and 1, 3, 5 and 7 days post-contact (DPC) from contact pigs. Five

inoculated pigs per group were necropsied at 3, 5 and 14 or 17 DPI. The five contact pigs were necropsied at 12 or 15 DPC. Bronchoalveolar lavage fluid (BALF) was collected from inoculated pigs at necropsy on 3 and 5 DPI. Sera were obtained from inoculated pigs and contact pigs at necropsy. All pigs were cared for in compliance with the Institutional Animal Care and Use Committee of the National Animal Disease Center.

H5 2.3.4.4-lineage specific RRT-PCR

The real-time RT-PCR targeting IAV H5 2.3.4.4-lineage viruses assay generates a 115 bp amplicon using two forward primers H5+800/T and H5+800/A (5′- GAG AGT AAT GGA AAT TTY ATT GCT CC-3′ and 5′- GAG AGT AAT GGA AAT TTY ATT GCA CC-3′, respectively), reverse primer H5–915 (5′- GTT TGA CAT TTG GTG TTG CA-3′), and the detection probe H5+855 (5′-[FAM]- GGG ACT CAA CAA TYA TGA AAA GTG -[NFQ]-3′). Y (C or T) indicates positions with multiple nucleotides. AgPath-ID One-Step RT-PCR kit was used to prepare a 25 µl reaction mixture using 1 µl of kit-supplied enzyme mix, 12.5 µl of kit-supplied buffer (2X), 5 pmol each of forward primers and detection probe and 10 pmol of reverse primer. The RT step conditions were 10 min at 45°C and 10 min at 95°C followed by two-step PCR cycling for 40 cycles of 94°C for 10 sec, 57°C for 30 sec, and 72°C for 10 sec. Fluorescence data were acquired at the end of the annealing step.

Positive sample metagenomic sequencing and analyses

Briefly, cDNA libraries for MiSeq were generated using the Nextera XT DNA Sample Preparation Kit (Illumina, https://www.illumina.comExternal Link) and sequenced using the 500 cycle MiSeq Reagent Kit v2 (Illumina) according to manufacturer instructions. De novo and directed assembly of genome sequences was performed using IRMA version 0.6.7, followed by visual verification in DNAStar SeqMan version 14 (https://www.dnastar.com) as needed. For each of the samples, variant calling was conducted by trimming raw FASTQ files using Trimmomatic using a sliding window size of 5 bp, a minimum Q-score of 30, and reads that were trimmed to a length shorter than 100 bases were discarded (*2*). These reads were aligned to reference sequences using bowtie2 v2.3.2 (*3*), duplicate reads were removed using Picard. The BAM files were converted to mpileup with samtools (*4*), and within-host variants were identified using VarScan (*5*). For a variant to be reported, we required the sequencing depth to be 100x, PHRED quality scores of 30, and to be detected at a frequency of at least 1% following thresholds that have been applied in prior studies (*6*). Nonsynonymous changes and those that

had been associated with a functional change were annotated with the results provided for each strain: the HA gene was annotated using H5 numbering including the signal peptide.

Microscopic lesion score

Microscopic lesion score was performed as previously described (*7*,*8*). Five parameters were evaluated per lung section: necrotizing bronchitis and bronchiolitis, suppurative bronchitis and bronchiolitis, peribronchiolar and perivascular lymphocytic infiltrates, alveolar septal inflammation and alveolar cellular exudate, edema, and hemorrhage. A composite score was computed with the sum of the five individual scores (0–20) (*7*). Two parameters were evaluated per tracheal section: epithelial degeneration and necrosis and inflammatory infiltrate for a possible composite score of 0–8 (*8*). Microscopic lesions were considered consistent with IAV infection if the microscopic lesion score was greater than 6 (lung) or 5 (trachea) and IAV was detected via PCR in BALF.

Immunohistochemistry

Heat-induced epitope retrieval was performed in an EZ-Retriever® IR System (BioGenex, Fremont, CA) using a citrate buffer (pH 6.0; Abcam) heated to 95°C for 2 cycles of 10 minutes. Slides were allowed to cool for 20 minutes followed by a rinse with deionized water and Dako Wash Buffer (2 × 5 min; Agilent). Slides were then incubated with hydrogen peroxide (3% in PBS; 2 X 8 minutes) to quench endogenous peroxidase activity, washed, and blocked for 60 minutes with 10% goat serum diluted in Dako Wash Buffer. Slides were incubated at room temperature for 60 minutes with primary antibody (1:2000) diluted in antibody dilution buffer (Agilent), followed by a secondary antibody (EnVision+ anti-rabbit Poly-HRP-IgG; Agilent) for 30 minutes. Diaminobenzidine chromogen detection was completed using Dako DAB Plus (5 min; Agilent) and Dako DAB Enhancer (3 min; Agilent). Slides were then rinsed with deionized water, cleared through gradient alcohol and xylene, counterstained using hematoxylin and coverslipped. Sections were examined by a veterinary pathologist (BA) using an Olympus BX43 light microscope. Photomicrographs were taken using an Olympus DP28 camera. Lung (conducting airways and alveolar lumen and septa) and tracheal immunohistochemical (IHC) score was recorded for each section as previously described (*9*).

Results

Mammalian and avian isolate within-host diversity was dominated by low-frequency variation

We identified 276 SNVs in the A/redfox/MI/22 (170 nonsynonymous, 102 synonymous, 4 missense), 203 SNVs in A/raccoon/WA/22 (120 nonsynonymous, 77 synonymous, 6 missense), 139 SNVs in A/bald eagle/FL/22 (87 nonsynonymous, 51 synonymous, 1 missense), and 51 SNVs in A/turkey/MN/22 (29 nonsynonymous, 22 synonymous).

References

1. Youk S, Torchetti MK, Lantz K, Lenoch JB, Killian ML, Leyson C, et al. H5N1 highly pathogenic avian influenza clade 2.3.4.4b in wild and domestic birds: introductions into the United States and reassortments, December 2021–April 2022. Virology. 2023;587:109860. **PMID 37572517**

2. Bolger AM, Lohse M, Usadel B. Trimmomatic: a flexible trimmer for Illumina sequence data. Bioinformatics. 2014;30:2114–20. PubMed https://doi.org/10.1093/bioinformatics/btu170

3. Langmead B, Salzberg SL. Fast gapped-read alignment with Bowtie 2. Nat Methods. 2012;9:357–9. PubMed https://doi.org/10.1038/nmeth.1923

4. Li H, Handsaker B, Wysoker A, Fennell T, Ruan J, Homer N, et al.; 1000 Genome Project Data Processing Subgroup. The Sequence Alignment/Map format and SAMtools. Bioinformatics. 2009;25:2078–9. PubMed https://doi.org/10.1093/bioinformatics/btp352

5. Koboldt DC, Chen K, Wylie T, Larson DE, McLellan MD, Mardis ER, et al. VarScan: variant detection in massively parallel sequencing of individual and pooled samples. Bioinformatics. 2009;25:2283–5. PubMed https://doi.org/10.1093/bioinformatics/btp373

6. Moncla LH, Bedford T, Dussart P, Horm SV, Rith S, Buchy P, et al. Quantifying within-host diversity of H5N1 influenza viruses in humans and poultry in Cambodia. PLoS Pathog. 2020;16:e1008191. PubMed https://doi.org/10.1371/journal.ppat.1008191

7. Morgan SB, Hemmink JD, Porter E, Harley R, Shelton H, Aramouni M, et al. Aerosol delivery of a candidate universal influenza vaccine reduces viral load in pigs challenged with pandemic H1N1 virus. J Immunol. 2016;196:5014–23. PubMed https://doi.org/10.4049/jimmunol.1502632

8. Gauger PC, Loving CL, Khurana S, Lorusso A, Perez DR, Kehrli ME Jr, et al. Live attenuated influenza A virus vaccine protects against A(H1N1)pdm09 heterologous challenge without vaccine associated enhanced respiratory disease. Virology. 2014;471-473:93–104. PubMed https://doi.org/10.1016/j.virol.2014.10.003

9. Gauger PC, Vincent AL, Loving CL, Henningson JN, Lager KM, Janke BH, et al. Kinetics of lung lesion development and pro-inflammatory cytokine response in pigs with vaccine-associated enhanced respiratory disease induced by challenge with pandemic (2009) A/H1N1 influenza virus. Vet Pathol. 2012;49:900–12. PubMed https://doi.org/10.1177/0300985812439724

10. Arruda BL, Kanefsky RA, Hau S, Janzen GM, Anderson TK, Vincent Baker AL. Mucin 4 is a cellular biomarker of necrotizing bronchiolitis in influenza A virus infection. Microbes Infect. 2023;25:105169. PubMed https://doi.org/10.1016/j.micinf.2023.105169

Appendix 1 Table 1. RT-qPCR Ct value and pathologic data by group and pig identification*

Group	Pig ID	BALF IAV PCR Ct	BALF H5 2.3.4.4 PCR Ct	Weighted Macroscopic Lung Lesion Score	Microscopic Pneumonia Score (0–20)	Conducting Airway Lung IHC Score (0–4)	Non-conducting Airway Lung IHC Score (0–4)	Cumulative Lung IHC Score (0–8)	Microscopic Tracheitis Score (0–8)	Trachea IHC Score (0–4)
Negative control	797	Neg	Neg	0.00	1	0	0	0	0	0
Negative control	816	Neg	Neg	0.50	1	0	0	0	0	0
Negative control	817	Neg	Neg	0.00	1	0	0	0	0	0
Negative control	51	Neg	Neg	0.00	1	0	0	0	1	0
Negative control	52	Neg	Neg	0.00	0	0	0	0	1	0
Negative control	53	Neg	Neg	0.00	0	0	0	0	0	0
Negative control	54	Neg	Neg	0.00	0	0	0	0	0	0
Negative control	55	Neg	Neg	0.00	1	0	0	0	0	0
Turkey DPI 3	776	Neg	Neg	0.20	0	0	0	0	0	0
Turkey DPI 3	777	29.3	29.5	7.10	6	0	0	0	0	0
Turkey DPI 3	778	29.6	31.3	0.00	2	0	0	0	0	2
Turkey DPI 3	779	35.0	37.9	1.20	2	0	0	0	0	0
Turkey DPI 3	780	Neg	Neg	0.00	1	0	0	0	0	0
Turkey DPI 5	781	29.2	30.5	0.00	0	0	0	0	0	0
Turkey DPI 5	782	Neg	Neg	0.00	0	0	0	0	0	0
Turkey DPI 5	783	34.3	Neg	0.00	0	0	0	0	0	0
Turkey DPI 5	784	30.1	30.9	0.70	0	0	0	0	0	1
Turkey DPI 5	785	Neg	Neg	0.00	1	0	0	0	0	0
Bald eagle DPI 3	791	25.5	26.5	2.03	8	3	1	4	5	1
Bald eagle DPI 3	792	29.3	31.6	3.38	8	2	1	3	4	3
Bald eagle DPI 3	793	35.3	39.5	0.00	1	0	0	0	0	0
Bald eagle DPI 3	794	24.6	25.2	1.55	16	4	3	7	10	4
Bald eagle DPI 3	795	36.0	36.4	0.20	1	0	0	0	0	0
Bald eagle DPI 5	796	21.4	22.7	4.70	18	4	4	8	12	0
Bald eagle DPI 5	798	22.9	24.2	0.20	11	3	3	6	9	1
Bald eagle DPI 5	799	24.3	25.4	1.80	3	1	1	2	3	3
Bald eagle DPI 5	800	25.2	25.8	0.70	12	4	3	7	10	1
Bald eagle DPI 5	818	22.4	25.5	1.00	0	0	0	0	0	4
Raccoon DPI 3	56	34.7	31.9	0.40	0	0	0	0	1	0
Raccoon DPI 3	57	Neg	Neg	0.28	0	0	0	0	0	0
Raccoon DPI 3	58	18.6	18.2	3.70	16	4	3	7	2	1
Raccoon DPI 3	59	27.7	26.3	0.00	3	0	0	0	5	1
Raccoon DPI 3	60	28.2	27.9	0.50	11	2	1	3	5	1
Raccoon DPI 5	61	25.8	24.1	0.00	1	0	0	0	0	0
Raccoon DPI 5	62	28.1	26.3	0.00	1	0	0	0	0	0
Raccoon DPI 5	63	27.8	26.5	0.20	2	0	0	0	4	1
Raccoon DPI 5	64	29.6	28.3	0.00	7	0	0	0	2	2
Raccoon DPI 5	65	32.3	30.8	0.00	2	0	0	0	1	1
Redfox DPI 3	76	37.1	36.2	3.20	11	3	2	5	3	1
Redfox DPI 3	77	28.1	31.1	2.58	10	3	1	4	4	1
Redfox DPI 3	78	34.1	30.7	4.33	10	3	1	4	5	2
Redfox DPI 3	79	34.2	32.9	1.33	1	0	0	0	2	1
Redfox DPI 3	80	25.0	21.1	0.28	1	0	0	0	0	0
Redfox DPI 5	81	23.6	22.4	3.55	3	0	0	0	3	2

Group	Pig ID	BALF IAV PCR Ct	BALF H5 2.3.4.4 PCR Ct	Weighted Macroscopic Lung Lesion Score	Microscopic Pneumonia Score (0–20)	Conducting Airway Lung IHC Score (0–4)	Non-conducting Airway Lung IHC Score (0–4)	Cumulative Lung IHC Score (0–8)	Microscopic Tracheitis Score (0–8)	Trachea IHC Score (0–4)
Redfox DPI 5	82	30.7	28.1	0.00	2	0	0	0	3	1
Redfox DPI 5	83	27.7	26.3	1.43	3	1	1	2	3	1
Redfox DPI 5	84	Neg	Neg	0.28	1	0	0	0	3	0
Redfox DPI 5	85	28.8	27.7	1.78	7	2	2	4	1	0

*BALF, bronchoalveolar lavage fluid; Ct, cycle threshold; DPI, days postinoculation; IAV, influenza A viruses; IHC, immunohistochemistry.

Appendix 1 Table 2. qRT-PCR positive samples successfully sequenced by group and animal identification*

	BALF DPI		Nasal Swab DPI/DPC			
Group	3	5	1	3	5	7
Turkey		781, 784				
Bald eagle	791, 792, 793, 794	796, 798, 799, 800 818				
Raccoon	58, 59, 60	63, 65	61	61	61, 65	67, 69
Redfox	77, 78, 79, 80, 81	82, 83, 84		85, 86		

*BALF, bronchoalveolar lavage fluid; DPI, days postinoculation; DPC, days postcontact; qRT-PCR, quantitative reverse transcription PCR.

Appendix 1 Table 3. Influenza A virus mean RT-qPCR Ct values and mean viral titer of lung homogenate of a swine-adapted H1N1*

	Right Cranial Lung		Left Cranial Lung		Caudal Lung (Right or Left)		% Positive
DPI	PCR Ct Value	Viral Titer	PCR Ct Value	Viral Titer	PCR Ct Value	Viral Titer	Pigs
3	23.0 ± 1.0	6.5 ± 2.0	22.8 ± 1.1	6.3 ± 1.9	25.7 ± 1.2	5.0 ± 2.0	100
5	24.0 ± 1.4	5.3 ± 2.8	25.7 ± 1.7	5.3 ± 1.9	24.9 ± 1.3	5.6 ± 2.7	100

*Eight pigs per necropsy time point, infected with the same device and approximate dose of a swine-adapted influenza A virus strain (subtype H1N1, A/swine/Iowa/A02429950/2019, HA clade 1A.3.3.3) of a former study included for comparison (*10*). Ct, cycle threshold; DPI, days postinoculation.

Appendix 1 Table 4. Influenza A virus mean RT-qPCR Ct values and mean viral titer of nasal swab samples of a swine-adapted H1N1*

DPI	PCR Ct Value	Viral Titer	% Positive Pigs
1	30.4 ± 3.3	3.4 ± 1.4	100
3	28.5 ± 1.3	3.8 ± 0.9	100
5	28.8 ± 1.4	3.8 ± 1.0	100

*24 (day post-inoculation 1), 16 (day post-inoculation 3) and eight pigs (day post-inoculation 5), infected with the same device and approximate dose of a swine-adapted influenza A virus strain (subtype H1N1, A/swine/Iowa/A02429950/2019, HA clade 1A.3.3.3) of a former study included for comparison (*10*). Ct, cycle threshold; DPI, days postinoculation.

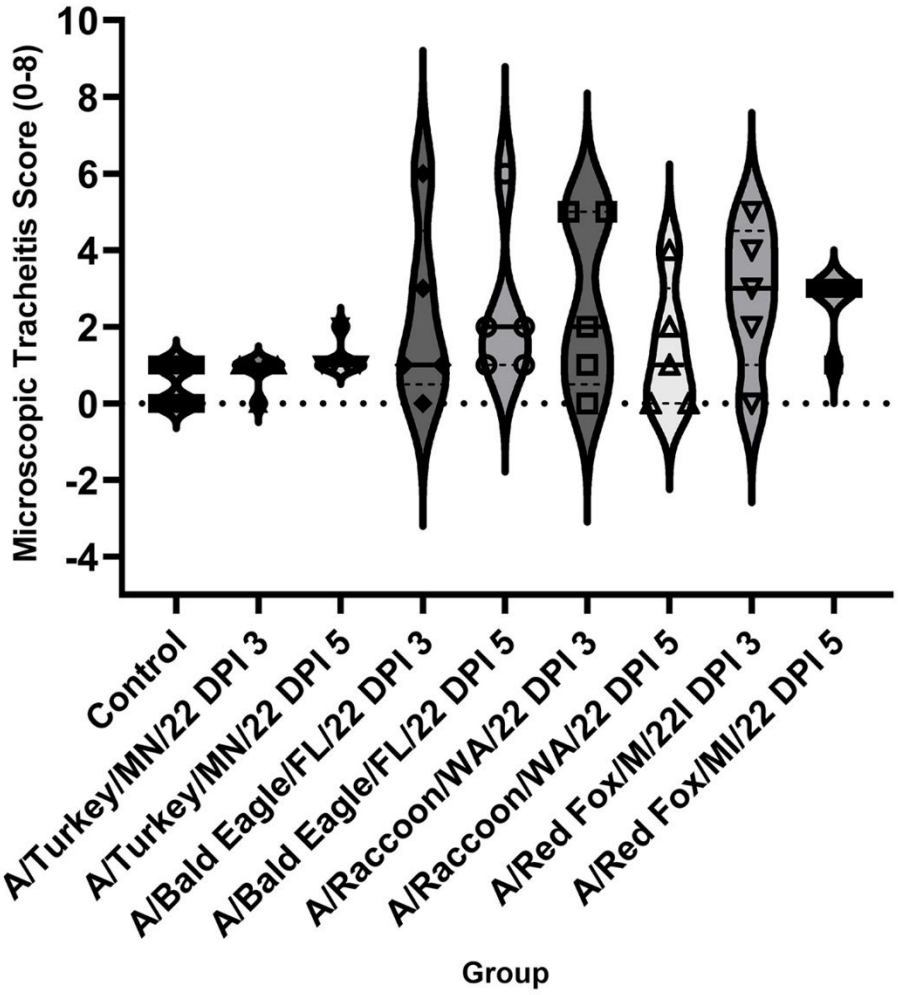

Appendix 1 Figure 1. Microscopic tracheitis score by strain and day post-inoculation (DPI). Median (solid line), quartiles (dashed line), and individual pig values (symbol) depicted. No statistically significant difference detected between strains by DPI.

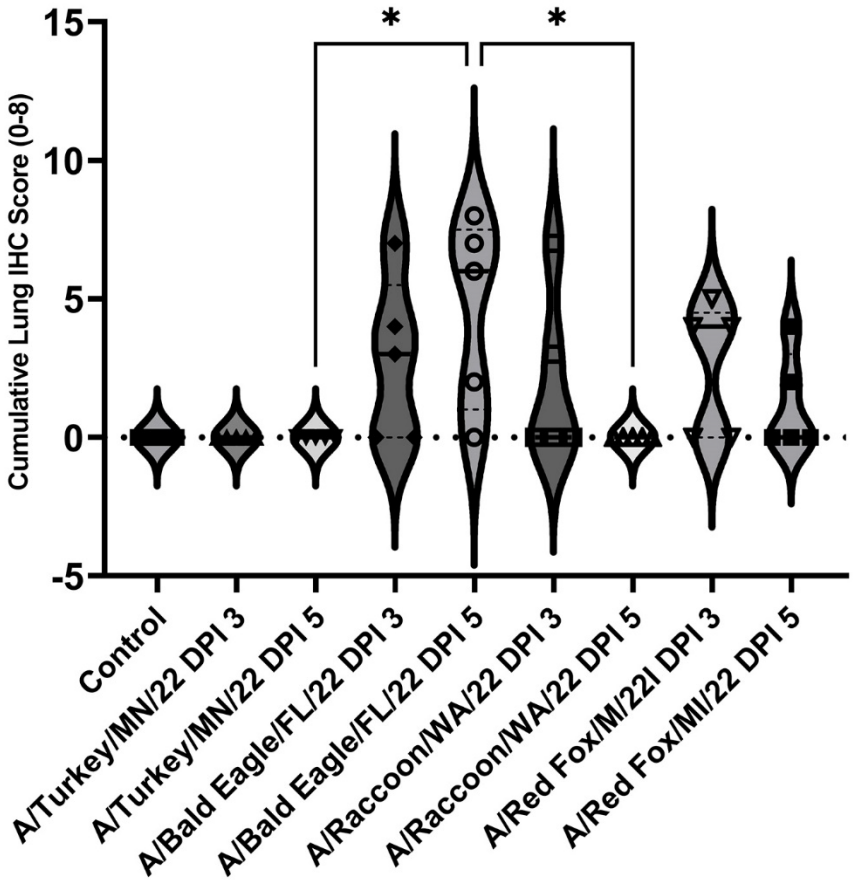

Appendix 1 Figure 2. Cumulative lung immunohistochemical score by highly pathogenic avian influenza strain and day post-inoculation (DPI). Median (solid line), quartiles (dashed line), and individual pig values (symbol) depicted. *$p < 0.05$.

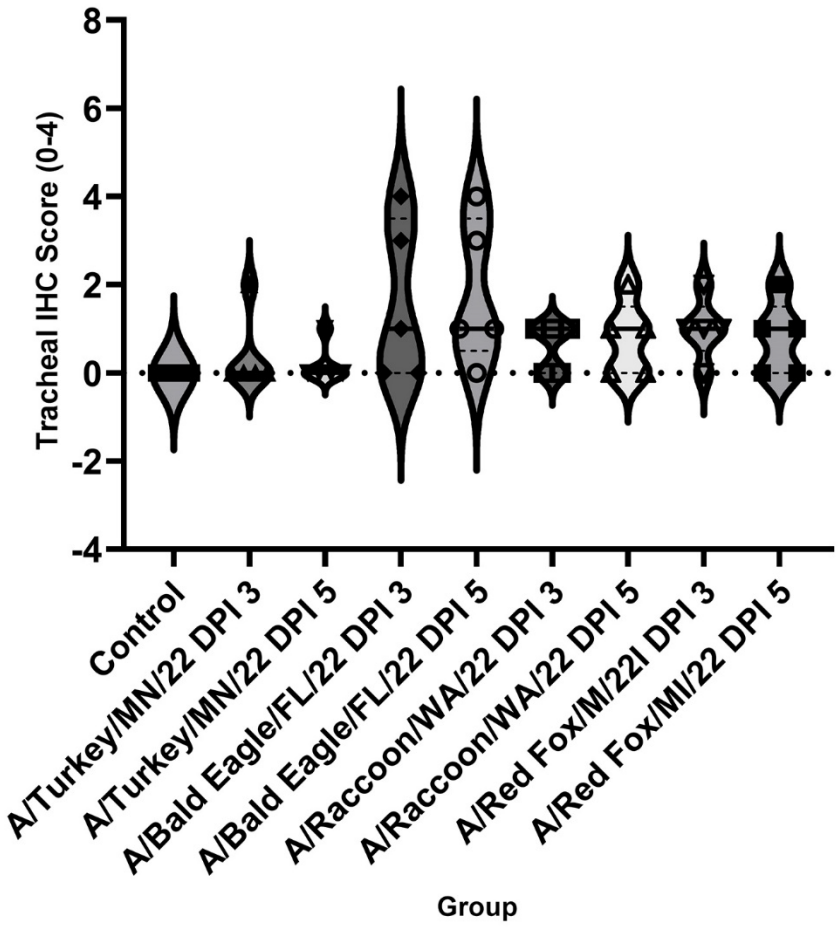

Appendix 1 Figure 3. Tracheal immunohistochemical score by highly pathogenic avian influenza strain and day post-inoculation (DPI). Median (solid line), quartiles (dashed line), and individual pig values (symbol) depicted. No statistically significant difference detected between strains by DPI.